 doi:10.20944/preprints202202.0041.v1

Article

Comparative Analysis on the Effect of Surface Reflectance for Laser 3D Scanner Calibrator

Jia Ou [1,2], Tingfa Xu [1,*], Xiaochuan Gan [2], Xuejun He [2], Yan Li [2], Jiansu Qu [2], Wei Zhang [2],Cunliang Cai [3]

1 School of Optics and Photonics, Beijing Institute of Technology, Beijing 100081, China; oujia100095@126.com (J.O.)
2 Beijing Changcheng Institute of Metrology and Measurement, Beijing 100095, China;9050432@qq.com (X.G.); 1587852073@qq.com (X.H.); liyanclei@163.com (Y.L.); qujiansu@163.com (J.Q.); 1194019406@qq.com (W.Z.)
3 School of Opto-electronic engineering, Changchun university of science and Technology, Changchun130022, China; caicunliang@126.com (C.C.)

* Correspondence: ciom_xtf1@bit.edu.cn (T.X.)

Abstract: The calibrator is one of the most important factors in the calibration of various laser 3D scanning instruments. The requirements for diffuse reflection surface are specially emphasized in many national standards. In this study, the spherical calibrator and plane calibrator comparative measurement experiments were carried out. The black ceramic standard sphere, white ceramic standard sphere, metal standard sphere, metal standard plane and white ceramic standard plane were used to test the laser 3D scanner. In the spherical calibrators comparative measurement experiments, the results indicated that the RMS of the white ceramic spherical calibrator with reflectance about 60% is 10 times that of the metal spherical calibrator with the reflectance of about 15%, and the RMS of the black ceramic spherical calibrator with reflectance of about 11% is of the same order as the metal spherical calibrator. In the plane calibrators comparative measurement experiments, the RMS of flatness measurement is 0.077 mm for metal plane calibrator with reflectance of 15%, and 2.915 mm for ceramic plane calibrator with reflectance of 60%. The results show that when the optimal measurement distance and incident angle are selected, the reflectance of the calibrator has a great effect on the measurement results, regardless of the outlines or profiles. Based on the experiments, it is recommended to use the spherical calibrator or the standard plane with reflectance of around 18% as the standard, which can obtain the reasonable results. In addition, it is necessary to clearly provide the material category and surface reflectance information of the standard when calibrating the scanner according to the measurement standard.

Keywords: Laser scanning instrument; 3D scanner calibrator; surface reflectance; measurement accuracy

1. Introduction

Non-contact measurement technology is widely used, especially for large-scale workpiece measurement, such as propeller blade [1], antenna reflector [2], cabin capacity [3][4], vertical metal container, etc. It can realize long-distance, high-precision and fast measurement for large-scale objects, which avoids interfacial contact and possible deformation in the measurement. Digital photogrammetry and scanning measurement methods are two important components in non-contact measurement. Digital photogrammetry mainly refers to the measurement technology, that utilizes digital cameras to obtain the images of the objects. After that these images were processed with further digital processing to obtain high-precision and three-dimensional (3D) contours of the measured objects' surface [5]. Generally, cooperative targets, such as marked points (reflective points or non-reflective points) and coding points need to be pasted on the surface of the measured object, which can be extracted by imaging processing software to measure the object.

Preprints (www.preprints.org) | NOT PEER-REVIEWED | Posted: 2 February 2022 doi:10.20944/preprints202202.0041.v1

Some laser 3D scanners generally do not need cooperative targets. The instrument projects visible features to the measured object. The common features include point, line [6], grating [7], speckle [8], and other different forms. For scanning measurement, the measuring light irradiates the surface of the measured object. The measured surface must be able to reflect a certain amount of light to ensure that the object surface contour can be obtained by reflected light. After being reflected by the measured surface, the imaging detector can precisely catch the light spot and then the position of the light spot was further processed and finally achieved the result.

3D scanning measurement instruments usually need to calibrate their accuracy before measurement. The common calibration method is to use a standard sphere with a certain diameter or a standard flat plane with a certain dimension. In practice, it is noted that the surface reflectance of the standard sphere/ plane has great influences on the accuracy of the measurement results. In order to reduce the effect of uneven reflection, powder spraying pretreatment is usually required in three-dimensional scanning operation, which can produce a dull and sub white coating on the workpiece. The spraying layer reduces the uneven reflectance of light and realizes much better scanning conditions. Spraying different powder has different effects on the surface reflectance. For instance, the size of titanium spraying powder is about 1 ~ 2um, and another kind of spraying powder size of DPT-5is about 5 ~ 6um [9-10]. Although spraying solves the issue on surface uneven reflectance, it alters the original surface roughness, as well as the size of the object. The calibrator for the measurement, whether it is a standard sphere or a standard plane, have strict geometrical tolerance and smooth surface roughness, which cannot be demonstrated with spraying powder. Therefore, it is necessary to study the effect of surface reflectance of the standard sphere or plane on the measurement results, looking for an appropriate surface reflection for direct application without spraying.

Facing this issue, some related parameters, such as color and light source that might affect the scanning measurement results, have been studied in reference [11-13]. In some typical applications, such as the influence of reflectance in laser 3D scanning of weld groove proposed by Andrej Cibicik et al. [14]. The change of reflectance produced more noise point cloud data. It is pointed out that when the light source is projected onto the metal surface, it may produce high intensity reflected light and light pollution, which affects the measurement results. That article also has given some methods to reduce the influence of noise. David A. Gonzalez et al. [15] mentioned the influence of surface reflectance and incident angle on surface measurement in the process of studying narrow angle flash nano-surface with reflectance suppression, and studied the method to reduce the influence of reflectance on measurement from the perspective of surface micro-nano structure. Tania Das et al. [16] also pointed out that incident angle and reflectance had a great impact on the measurement results when using polarized light to measure the surface topography of metal, and studied the method of using polarized light to detect the surface contour of metal plane. In many studies, the influence of reflectance on the measurement of laser scanning method has been found, but few studies have studied the influence of reflectance on the measurement accuracy from the perspective of calibration of laser scanner.

In this study, using a variety of materials with different surface reflectance, combined with scanning measurement tests, the effect of surface reflectance on the scanning measurement result is investigated. The experimental result might improve the current regulation of instrument calibration and provide some reference for the further study on the scanning measurement.

2. Methodology and Mechanism

2.1 Principle of laser scanning measurement

Preprints (www.preprints.org) | NOT PEER-REVIEWED | Posted: 2 February 2022 doi:10.20944/preprints202202.0041.v1

According to the number of scanning points at one time, the instruments can be classified into point scanning, linear scanning, and plane scanning. The point scanning method can only measure one point at one time because of the limitation of its distance measurement theory. Based on the principle of spherical coordinates, as shown in Figure 1, the position of point P (x, y, z) in the spherical coordinate can be obtained based on the radius *r*, azimuth α and elevation θ. The value of *r* can be obtained by collecting the duration of light travelling between instrument and the object, the value of α and θ be obtained by angle encoders in instrument. Point scanning system is commonly found in MV330/350 LASER RADAR produced by Nikon, Japan, which uses a ranging technology of frequency modulation coherent LIDAR technology [17], and ATS600 absolute tracker and various ground-based laser scanner produced by Leica, Germany.

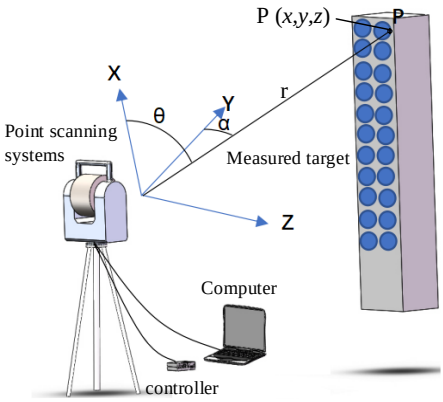

Figure 1. Schematic diagram of mechanism of single-point laser scanning measurement in spherical coordinate.

The line scanning method projects a single laser line or multiple laser lines to the measured surface, as shown in Figure 2. Numerous measure points along the line can be collected at one time. The number of points along the line scanning is related to the hardware of the scanning system [18]. The line scanning systems are commonly found in LJ-G5000 series laser 2D/3D high precision measurement systems produced by Keyence, Japan.

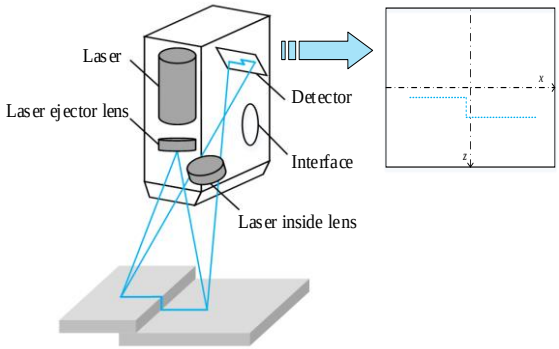

Figure 2. Schematic diagram of mechainsm of single-line laser scanning system.

Preprints (www.preprints.org) | NOT PEER-REVIEWED | Posted: 2 February 2022 doi:10.20944/preprints202202.0041.v1

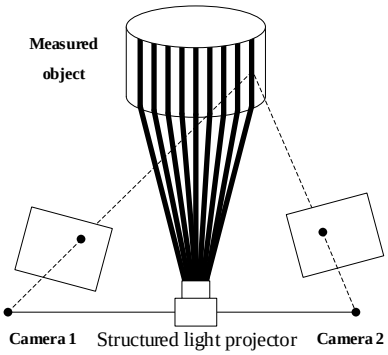

Figure 3. Schematic diagram of mechanism of stripe-area laser scanning system.

The area scanning system [11] projects grating, moire fringe, speckle and other different patterns onto the measured surface. In general, more measurement points can be obtained at one time than line scanning. The area scanning system makes use of stereo vision and structured light [19-20], as shown in Figure 3. The structured light is projected onto the surface of the measured object through the transmission of light source and a 3D image fitting the surface shape of the measured object is formed on its surface. The 3D image is captured by two cameras to obtain the distorted image modulated by object spatial dimension. The 3D point cloud information of the object surface is obtained for further image processing and the image point cloud is divided into fields by software [21-22]. The 3D geometric features are synthesized to re-construct the measured surface. The representative instruments are the ATOS series scanners produced by GOM, Germany and Combet series scanners produced by Zeiss company, Germany.

No matter what kind of laser scanner, its basic principle is that the receiving system receives the laser reflected light irradiated on the surface of the measured object. If the energy of reflected light is too low, the receiving signal constants lots of comparable noise from the surroundings. On the contrary, if the reflected light is over-strong, the receiving system may be saturated, resulting in wrong data. Therefore, if the laser scanner is calibrated, it is necessary to study the differences between standards with different reflectance and find a suitable reflectance standard sphere or standard plate.

2.2 Effect of incident angle and reflectance on 3D scanning

The laser scanner collects the 3D information of the objects through the point cloud data [23]. Theoretically, the difference can be achieved by comparing the measured data of the scanner with the known coordinate points. However, in practical application, it is difficult to have a sufficiently small object as the target point. Therefore, using the standard sphere and standard plane is a common method to calibrating the scanning system. The calibrated 3D scanning system constructs the point cloud data of the standard sphere to obtain the diameter of the standard sphere and then compares the data with the known radius of the standard sphere. Similarly, the data of the standard plane obtained by the calibrated scanning system can also be compared with the known data to judge the measurement accuracy of the 3D scanner system. In this way, whether it is a standard sphere or a standard plane, the reflection characteristics will affect the accuracy of the measurement results.

For different materials, the change trend between the laser incidence angle and the reflection intensity is similar. The reflection intensity can be determined by the relationship between the laser incidence angle and the reflection intensity [24].

The surface reflectance of the measured object is a key parameter related to the measurement ability of the laser scanner. The main factors affecting the reflectance of object surface are object surface color and surface type (matte, highlight, smooth, rough, etc.). It is generally defined that the surface reflectance of Kodak white material is 100%, and that of Kodak gray material is 18% [25]. In order to reduce the influence of reflectance on the

Preprints (www.preprints.org) | NOT PEER-REVIEWED | Posted: 2 February 2022 doi:10.20944/preprints202202.0041.v1

measurement results, the common method is to find a suitable incidence angle and provide a standard sphere or standard plane with appropriate reflectance.

3. Experiment

In order to research the effect of reflectance on the calibration result of scanner, white ceramic ball with higher reflectance, black ceramic ball with lower reflectance and metal ball with lower reflectance were made as standard spheres and their surface reflectance were determined. Firstly, two standard spheres with different reflectance of ceramic materials were tested and the radii of the two balls measured by the scanner were compared. The three standard spheres were then placed together to compare the material's effect on the scans. In order to exclude the influence of incident angle on the measurement results, we made low reflectance metal plane and high reflectance ceramic plane as the standard plane, to verify the influence of reflectance on the measurement results.

3.1 Reflectance measurement of the standard spheres

The measurement standard JJF 1032-2005, the definition of reflectance is given as follows: under the specified conditions of the spectral composition, polarization state, and geometric distribution of the incident radiation, the ratio of the reflected radiant flux to the incident flux. JJF 1232-2009 calibration specification for reflectance meter, which is used to measure the diffuse reflectance of paint, coating, ceramics and other materials. The reflectance of the most of the common materials can be obtained by such instruments.

In this study, a spectrophotometer (produced by SPECTRO, Germany) is used to measure the surface reflectance. The colorimeter adopts D/8 geometric optical structure [26-28], which is a diffuse reflection illumination, 8° detection method. 2°/10° standard observer angle, D65 standard light source is used for measurement. Specular component included (SCI) is a measurement mode that includes specular reflection light and SCE (specular component excluded) is a measurement mode that excludes specular reflection light. Finally, three standard surfaces are given, they are metal surface A, ceramics surface (black) B, and ceramics surface(white) C, the reflectance of standard spheres made by three different materials are shown in Tab.1. By measuring the reflectance, we obtained the reflectance of metal standard sphere and black ceramic sphere with similar reflectance and the reflectance of white ceramic sphere with relatively high reflectance. The experimental results can be used to compare different materials with similar reflectance and the same material with large difference reflectance.

Table 1. The reflectance of standard spheres made by three different materials.

NO.	Materials	Surface treatment	Surface reflectance
1	Metal	Matte	15%
2	Ceramics (Black)	Matte	11%
3	Ceramics (White)	Matte	60%

3.2 Calibration experiment of ceramic standard spheres scanning with large reflectance difference

In order to investigate the effect of surface reflectance on scanning measurement, the scanning tests were carried out to compare black standard ceramic sphere and white standard ceramic sphere respectively. The point scanning system (MV330/350 LASER RADAR) with the maximum permissible error (MPE) ±0.3 mm was used for scanning, two ceramic balls were scanned simultaneously under the same conditions to get the surface morphologies.

The test samples are chosen as black standard ceramic spheres (matte surface, reflectance of about 11%, the diameter is 101.600mm) and white ceramic balls (bright surface, reflectance of about 60%, the diameter is 100.000mm), respectively, as shown in the Figures 4 and 5. The distance between the ceramic ball and the scanning system is about 3 m.

Preprints (www.preprints.org) | NOT PEER-REVIEWED | Posted: 2 February 2022 doi:10.20944/preprints202202.0041.v1

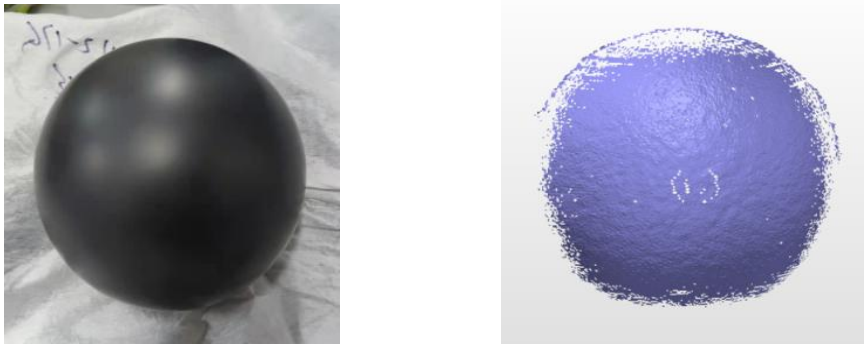

(**a**) (**b**)

Figure 4. (a) Photograph of the black standard ceramic sphere with matte surface, and (b) point cloud obtained by point scanning system.

Figure 4(b) present the measured results of the black standard ceramic sphere. The point cloud is shown using the best fitting sphere [29]. The fitting condition is that the maximum angle is 45°. The ratio of eliminating the noise is 5% and the same parameters were further employed in the following scanning tests. In the experiment, 25,298 points are obtained. According to the measured result, the fitted diameter is 101.488 mm, and the root mean square (RMS) is 0.013 mm. The experimental result indicates that the measured surface is relatively smooth and the surface roughness is within the accuracy of the instrument shown in Figure 4(b).

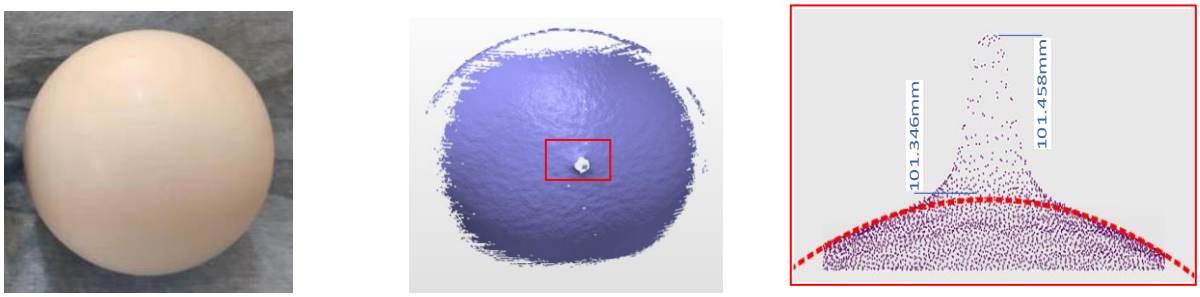

(**a**) (**b**) (**c**)

Figure 5. (a) White ceramic ball with bright surface with reflectance of about 90%, (b) point cloud data at vertical incidence, and (c) close view of the protrusion marked in (b).

Since the object to be measured is a sphere, the scanning system must have almost vertical incidence, for the measured ball with high reflectance, invalid data will appear. It can be seen from Figure 5(b) and 5(c), that when the incident angle is close to zero, some remarkable protrusions appear on the spherical surface, which is due to localized high reflectance. Based on the obtained data cloud (24,927 points), the fitting calculation diameter is 99.746 mm, and the RMS is 0.094 mm. From the measurement results, the RMS value of the black ceramic sphere with 11% reflectance is 0.013mm, and the diameter measurement difference is -0.112mm. Under the same measurement conditions, the RMS value of the white ceramic sphere with 60% reflectance is 0.094mm, and the diameter measurement difference is -0.254mm. During the experiment, we made many measurements, and the trend of the results is basically consistent with the above results. Namely, the measurement deviation and RMS value of the measured white ceramic sphere with high reflectance are much higher than that of the black ceramic sphere with low reflectance.

3.3 Standard spheres scanning calibration experiments for different materials and reflectance

In order to verify the influence of different materials on the scanning calibration results, three calibrated standard spheres were scanned simultaneously. As shown in Figure

Preprints (www.preprints.org) | NOT PEER-REVIEWED | Posted: 2 February 2022 doi:10.20944/preprints202202.0041.v1

6, the diameter of ball A is 101.600mm, the reflectance is 15%, and the material is metal. The diameter of ball B is 101.600mm, the reflectance is 11%, and the color and material are black and ceramic respectively. The diameter of ball C is 100.000mm, the reflectance is 60%, the color and material are white and ceramic respectively.

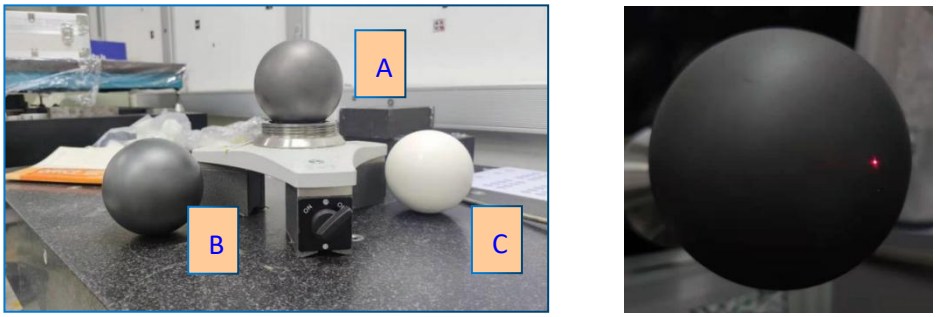

(**a**) (**b**)

Figure 6. Scanning measurement comparison based on different reflectance (a) the standard spheres made by three different materials with different reflectance, and (b) scanning light spot on black ceramic surface.

LIDAR scanner is used to scan the surface of three balls at approximately equal distances. The obtained point clouds for three balls is shown in Figure 7, and the re-constructed fitting spheres based on the three point clouds by the scanning are shown in Figure 8. From the scanning measurement data of different balls shown in the Tab.2, it can be seen that the RMS parameters of the white ceramic ball with reflectance of about 60% are 10 times higher than those of the metal ball with reflectance of about 15% and black ceramic ball with reflectance of about 11%, and the point cloud data measured by the metal ball have the smallest RMS parameters in the ball fitting. The RMS parameter of the black ceramic ball with reflectance of about 11% is of the same order of magnitude as that of the metal sphere, but the dimensional deviation is twice that of the metal ball.

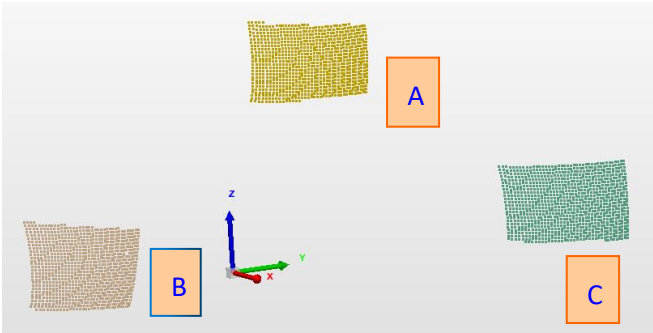

Figure 7. Point clouds obtained from laser scanning of the three balls.

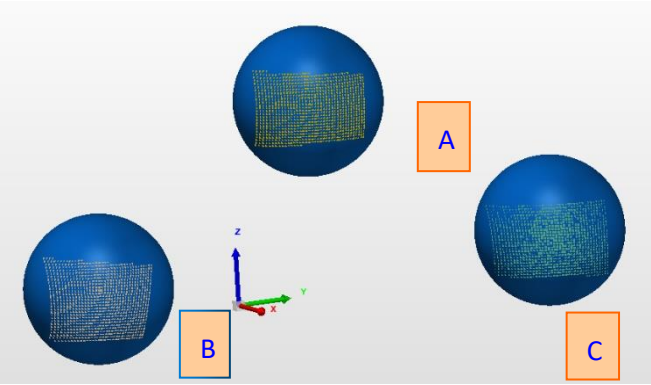

Preprints (www.preprints.org) | NOT PEER-REVIEWED | Posted: 2 February 2022 doi:10.20944/preprints202202.0041.v1

Figure 8. The re-construction based on the point clouds by the scanning measurements

Table 2. Comparison of LiDAR scanning 101.6 mm ball results

Materials	Pts	Diameter	Deviation	RMS	RMS Fixed radius
Metal	862	101.463	-0.137	0.009	0.011
Ceramics (Black)	949	101.313	-0.287	0.013	0.019
Ceramics (White)	892	99.709	-0.291	0.099	0.102

In order to verify the influence of different materials on the scanning calibration results, three calibrated standard spheres were scanned simultaneously. As shown in Figure 6, the diameter of ball A is 101.600mm, the reflectance is 15%, and the material is metal. The diameter of ball B is 101.600mm, the reflectance is 11%, and the color and material are black and ceramic respectively. The diameter of ball C is 100.000mm, the reflectance is 60%, the color and material are white and ceramic respectively.

Through the scanning calibration comparison experiment of metal standard sphere with similar reflectance, black ceramic standard sphere and white standard sphere with high reflectance, we find that there are slight differences in calibration results when materials are different and reflectance is similar. However, for the white standard sphere with 60% reflectance, the calibration result obviously has a large deviation.

3.4 Contrast experiment of plane scanning

When measuring spherical standard body, the laser scanner inevitably had the difference of incident angle. In order to exclude that the difference in the measurement results in the standard sphere calibration experiment was caused by the difference in incidence angle, we conducted a comparison experiment between the metal standard plane with a reflectance of 15% and the ceramic standard plane with a reflectance of 60% at a fixed incidence angle of 25°.

As shown in Figure 9, the metal plane with matte surface and reflectance of about 15% is selected as the test sample, and the working surface size is about 460 mm × 190 mm with 0.2 mm flatness. In addition, another sample is white ceramic plane with matte surface and reflectance of about 60%. The working surface size of about 450 × 80 mm with 0.01 mm flatness. The metal plane and white ceramic plane are 3 m away from the scanning system during scanning.

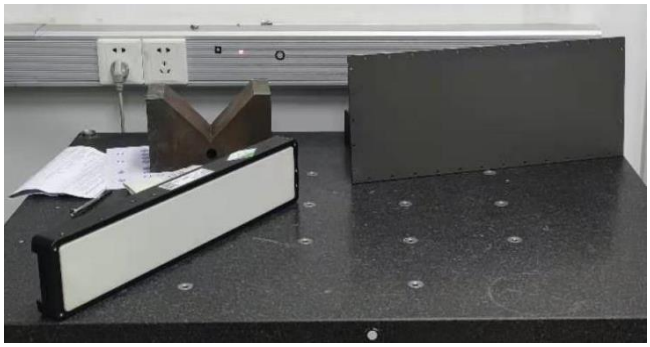

Figure 9. The photographs of the metal plane and white ceramics plane.

As shown in Figure 10, the measured surface is re-constructed by obtained point cloud shown using the best fitting plane. The fitting flatness of the measured plane is 0.345 mm with the number of points of 138,681, and the standard deviation and RMS are both 0.077mm. GD&T's evaluation standard uses ASME Y14.5 2009.

Preprints (www.preprints.org) | NOT PEER-REVIEWED | Posted: 2 February 2022 doi:10.20944/preprints202202.0041.v1

Figure 10. The re-construction of the metal plane based on the measured point cloud.

As shown in Figure 11, the calculation method of the best fitting plane is used to calculate the point cloud of the white ceramic plane, which includes 1,824 valid points. The fitting calculation result is that the flatness is 11.134 mm. The standard deviation and RMS are 2.916 mm and 2.915 mm, respectively. The evaluation standard of GD&T is ASME Y14.5 2009.

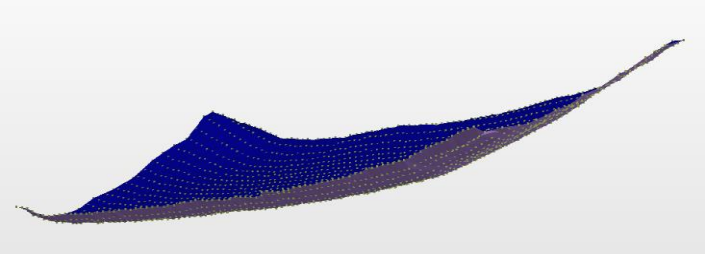

Figure 11. Triangular surface slice results of ceramic plane point cloud.

It can be concluded that high surface reflectance will adversely affect the measurement, for both spherical and plane object.

5. Conclusions

In order to investigate the effect of standard spheres or planes with different materials and reflectance on non-contact scanning measurement results during instrument calibration, point scanning systems were used to analyze and compare the scanning data of metal, black and white ceramic balls, white ceramic plane and gray metal plane with different reflectance. The performance of the instrument is found to be related to the surface. The RMS of the white ceramic ball with reflectance of about 60% are 10 times higher than those of the metal ball with reflectance of about 15%. So it is necessary that the information on the testing surface should be given to facilitate intercomparison between different instruments for instrument calibration.

Author Contributions: Conceptualization, J.O. and T.X.; methodology, X.G. and W.Z. ; software, J.Q.; validation, T.X., X.H.; formal analysis, J.O.; investigation, X.G.; resources, C.C.; data curation, Y.L.; writing—original draft preparation, J.O.; writing—review and editing, C.C.; visualization, C.C.; supervision, T.X.; project administration, J.O.; All authors have read and agreed to the published version of the manuscript.

Funding: Not applicable

Institutional Review Board Statement: Not applicable

Informed Consent Statement: Not applicable

Data Availability Statement: Not applicable

Acknowledgments: Not applicable

Conflicts of Interest: The authors declare no conflicts of interest.

References

1. Wei, Y.; Deng C.; Wu, X.; Ao, L. Three dimensional measurement system for the dynamic deformation of aero-engine blade profile. *INT. J. ARTIF. INTELL. T*. **2020,** *29(7n08)*, 2040014.
2. Yang, J.; Qi, S.; Wu, W.; Fang, D. A novel sum and difference conical beam-scanning reflector antenna. *IEEE ACCESS*. **2020,** *PP(99)*, 1-1.
3. Zhu, W.; Qi, G.; Zhang, Q.; Wang, Y. Ou, J. A non-contact measurement method of cabin capacity based on structured light vision. *2016 IEEE Int. Conf. Mech. and Automat.* **2016**.
4. Goba, I.; L'Hostis G.; Guerlain, P. In-situ non-contact 3D optical deformation measurement of large capacity composite tank based on close-range photogrammetry. *OPT. LASER. ENG.* **2019,** *119(AUG.)*, 37-55.
5. Gong, Q.; Zhu, B. Application analysis of three-dimensional laser scanning technology in engineering surveying and mapping. *World Nonferrous Metals*. **2019**.
6. Ma, Q.; Zhang, D.; Jin, S.; Ren, Y.; Li, Y. On Path Generation Method for Laser Cleaning Robot Based on Line Structured Light. *2020 29th C.C.C.* **2020**.
7. Tang, Q.; Zhang, G.; Zhang, C.; Zhao, B. Reflection grating spectrometer based on AOTF. *Sixth Symposium on Novel Photoelectronic Detection Technology and Application*. **2020,** *11455*, 114555Y.
8. Miao, C.; Tippur, H. V. A simplified reflection-mode digital gradient sensing technique for measuring surface slopes, curvatures and topography. *OPT. LASER. ENG*. **2020,** *124(Jan.)*, 105843.1-105843.13.
9. Wang, R.; Law, A.; Kong, Z.; Garcia, D.; Yang, S. Development of structured light 3d-scanner with high spatial resolution and its applications for additive manufacturing quality assurance. *INT. J. ADV. MANUF. TECH.* **2021**.
10. Li, W.; Fan, J.; Li, S.; Tian, Z.; Yang, J. Calibrating 3d scanner in the coordinate system of optical tracker for image-to-patient registration. *FRONT. NEUROROBOTICS.* **2021,** 15.
11. Li, F.; Li, H.; Kim, M. K.; Lo, K. C. Laser scanning based surface flatness measurement using flat mirrors for enhancing scan coverage range. *REMOTE SENS-BASEL.* **2021,** *13(4)*, 714.
12. Zaimovic-Uzunovic, N.; Lemes, S. Influences of Surface Parameters On Laser 3D Scanning. *IMEKO Conference Proceedings: International Symposium on Measurement and Quality Control: Osaka, Japan*. **2010,** D024-026.
13. Wen, Y.; Hu, J.; Pagilla, P. R. A Novel Robotic System for Finishing of Freeform Surfaces. *Int. Conf. Robot. and Automat.* **2019,** 5571-5577.
14. Andrej C.; Lars T.; Olav E. Laser Scanning and Parametrization of Weld Grooves with Reflective Surfaces. *Sensors.* **2021,** 21,479.
15. David A. G.; Jesus M.; David S.; Karun V.; Menelaos K. P. Narrow-angle scatter of reflectivity-suppressing nanostructured surfaces. *Optical Engineering.* **2020,** 59(10), 1031061-10310613.
16. Tania D.; Kallol B. Topometry of metal surfaces using reflection of polarized light. *Optik.* **2021,** 167448.
17. Amzajerdian, F. Analysis of Technology for Compact Coherent Lidar (13 Aug. 1996- 30 Jun. 1997). **1997**.
18. Pose calibration for 2d laser profiler integrated in five-axis machine tools. *IOP Conference Series: Materials Science and Engineerin*. **2020,** *831(1)*, 012022
19. Madhusudanan, H.; Liu, X.; Chen, W.; Li, D.; Sun, Y. Automated Eye-in-Hand Robot-3D Scanner Calibration for Low Stitching Errors. *2020 IEEE Int. Conf. Robot. and Automat*. **2020,** 8906-8912.
20. Xue, J.; Li, G.; Wang, Z.; Xie, X. A novel stripe extraction scheme for the multi-line structured light systems. *2021 IEEE Int. Symp. Circ. and Syst.* **2021,** 1-5.
21. Oh, S. H.; Park, J. S.; Ryu, J. J.; Song, I. S.; Jung, S. K. Three-dimensional reproducibility of the soft tissue landmarks taken by structured-light facial scanner in accordance with the head position change. *HEALTHCARE-BASEL*. **2021,** *9(4)*, 428.
22. Tian, B. Application of terrestrial laser scanning (tls) in the architecture, engineering and construction (aec) industry. *SENSORS-BASEL*. **2021,** *22(1)*, 265.
23. Carrea, D.; Abellan, A.; Humair, F.; Matasci, B.; Derron, M. H.; Jaboyedoff, M. Correction of terrestrial lidar intensity channel using oren–nayar reflectance model: an application to lithological differentiation. *ISPRS. J. PHOTOGRAMM.* **2016,** *113*, 17-29.
24. Xia, G. F.; Chun-Mei, H. U.; Cao, B. Z.; Tian-Shuo, L. I. Study on the influence of laser incident angle on the reflection intensity of the point cloud. *Laser Journal*. **2016,** *37(04)*, 11-13. (in Chinese)
25. Tirelli, C.; Manzo, C.; Curci, G.; Bassani C. EVALUATION OF THE AEROSOL TYPE EFFECT ON THE SURFACE REFLECTANCE RETRIEVAL USING CHRIS/PROBA IMAGES OVER LAND. *The 36th International Symposium on Remote Sensing of Environment*. **2015**.
26. MUKUPA, W.; ROBERTS, W. R.; HANCOCK, C. M.; ALMANASIR, K. Correction of Terrestrial LiDAR Data Using a Hybrid Model. *FIG Working week*. **2017**.
27. Shourt, W. V.; Besuner, R.; Silber, J.; Dunlop, P.; Tarle, G. Precision alignment and integration of DESI's focal plane using a laser tracker. *Ground-based and Airborne Telescopes VIII*. **2020**.
28. Nfmk, A.; Pm, B.; Res, A.; Ejwa, B.; Mpb, C. Assessing firmness in mango comparing broadband and miniature spectrophotometers - sciencedirect. *INFRARED PHYS. TECHN.* **2021,** 115.
29. Pan, B. Z.; Tang, J. Best-fitting sphere of aspheric surface based on spherical aberration. *OPT. REV.* **2020,** *27(11)*.